# Brazovskii-Dyugaev effect on the inhomogeneous chiral transition in quark matter



Karasawa, Shintaro; Lee, Tong Gyu; Tatsumi, Toshitaka

PTEP

Prog. Theor. Exp. Phys. **2016**, 043D02 (21 pages)
DOI: 10.1093/ptep/ptw025

# Brazovskii–Dyugaev effect on the inhomogeneous chiral transition in quark matter

Shintaro Karasawa*, Tong-Gyu Lee*, and Toshitaka Tatsumi*

*Department of Physics, Kyoto University, Kyoto 606-8502, Japan*
*E-mail: karasawa@ruby.scphys.kyoto-u.ac.jp, lee@ruby.scphys.kyoto-u.ac.jp, tatsumi@ruby.scphys.kyoto-u.ac.jp

Received January 18, 2016; Revised February 16, 2016; Accepted February 17, 2016; Published April 15, 2016

We investigate the effects of quantum and thermal fluctuations on the phase boundary between the inhomogeneous chiral phase and the chiral-restored phase in the phase diagram in the plane of temperature and chemical potential. Introducing the composite fields made of quark bilinear fields, we construct an effective action for them in quark matter by way of the correlation function method. Utilizing this effective action, we discuss the effects of the quark–antiquark and particle–hole pair fluctuations to find possible modifications of the vertex functions of the order parameter included in the thermodynamic potential. We find that the most important effect of the pair fluctuations is to change the sign of the fourth-order vertex function to make the phase transition always the first, rather than the second, order (we call it the *Brazovskii–Dyugaev* effect). Another important effect manifests in the second-order vertex function: it exhibits a singular behavior near the critical point, which prohibits the second-order phase transition. It, together with the fourth-order vertex function, alters the location of the phase boundary.

Subject Index D30

## 1. Introduction

A full understanding of a phase structure for quantum chromodynamics (QCD) in the plane of temperature ($T$) and chemical potential ($\mu$) is among the ultimate goals in high energy nuclear and hadron physics (see, e.g., [1] for a recent review). In recent theoretical investigations of QCD at moderate densities, there has been a growing number of studies focusing on inhomogeneous chiral condensates [2–12] which are spatially modulated with finite total momentum in analogy with charge and spin density waves [13–16] or Fulde–Ferrell–Larkin–Ovchinikov states [17,18]. The presence of inhomogeneous chiral phases may extend the chiral-broken regime and thereby could delay the complete restoration of chiral symmetry as well, dramatically refreshing the conventional QCD phase diagram (see [19] for a review).

The fundamental concept of the inhomogeneous chiral order parameter is presented by generalizing the usual (homogeneous) one. Considering the chiral $SU(2)_L \times SU(2)_R$ symmetry and introducing the composite fields made of the quark bilinear fields, $\phi_0 \sim \bar{\psi}\psi$ and $\phi_i \sim \bar{\psi}\gamma_5\tau_i\psi$ with the light quark fields $\psi$ and the $SU(2)$ generators $\tau_i$, we define a spatially modulated order parameter such as $\Phi(z) \equiv \langle\phi_0(z)\rangle + i\langle\phi_3(z)\rangle \equiv \Delta(z)e^{i\theta(z)}$, where $\Delta(z)$ and $\theta(z)$ are the modulated amplitude and phase in the $z$-direction, respectively. This corresponds to a one-dimensional modulation embedded

in 1+3 dimensions[1] and can be classified in the context of the phase modulation and the amplitude modulation, i.e., $\Phi(z) = \Delta e^{iqz}$ and $\Phi(z) = \Delta(z)$; the former is called the dual chiral density wave (DCDW) [4] and the latter the real kink crystal (RKC) [8].

Earlier studies about inhomogeneous chiral phases so far have been restricted to special situations such as vanishing current quark masses, zero magnetic fields, no fluctuations, and so forth. However, more elaborate studies are needed to fully understand the inhomogeneous chiral transition and discuss its phenomenological implications. Recently, there have been growing attempts to incorporate various elements to this end.[2] For the effect of the current quark mass, there are some differences between the DCDW phase and the RKC phase; the exact solution is obtained for the RKC phase in a self-consistent treatment [7,26], while for the DCDW phase the corresponding solutions are approximately achieved by using a perturbative method [27] or a variational method [28,29]. In particular, for the DCDW case, it has been shown that finite current mass gives rise to a modification of the function form of the inhomogeneous condensate. A nonzero magnetic field extends the DCDW phase to the wide region [30,31]. This is because an anomalous baryon number is induced due to the spectral asymmetry of the lowest Landau level [32]. A new type of condensate, the hybrid chiral condensate, may also be realized there [31], which is akin to the so-called twisted kink crystal [33]. As another interesting possibility, there is a recent work [34] that discusses the spontaneous magnetization stemming from the spectral asymmetry. For the effect of the fluctuations in the DCDW phase, it has been shown that thermal fluctuations lead to a Landau–Peierls instability [35] and thus wash out the long-range order [36]. However, an algebraically decaying (quasi-long-range) order remains (see also [37] for the RKC phase).

In this paper, we focus on another effect of the fluctuations around the order parameter in the inhomogeneous chiral transition: $\phi_a(t, \mathbf{r}) = \langle \phi_a(t, \mathbf{r}) \rangle + \delta\phi_a(t, \mathbf{r})$ with $a = 0 \sim 3$, where the symbol $\langle \cdots \rangle$ means the thermal average and $\delta\phi_a(t, \mathbf{r})$ is the fluctuation field. We, hereafter, consider the quark–antiquark and particle–hole pair fluctuations (we call them the "chiral pair fluctuations" in this paper) in the chiral-restored phase to discuss the fluctuation-induced phase transition. In general, quantum and/or thermal fluctuations around the spatially modulated order parameter can change the order of the phase transition due to the peculiar form of the propagator $G(q_0, \mathbf{q})$ of the fluctuation field near the transition point, which differs from the usual one in holding a nonzero momentum, $|\mathbf{q}| = |\mathbf{q_c}| = q_c$. This was first shown by Brazovskii [38], who pointed out that thermal fluctuations change the coefficients of the terms in each order of $\langle \phi_a(z) \rangle$ in the thermodynamic potential, which implies that the phase transition between spatially homogeneous and inhomogeneous phases becomes of the first order rather than of the second order. Such an effect is called the *Brazovskii effect*, which has been refined and applied to systems that undergo a phase transition to a spatially inhomogeneous state, e.g., soft matter systems [39,40], and also has been experimentally confirmed in diblock copolymers [41]. Dyugaev [42], on the other hand, has discussed that quantum fluctuations also exhibit the same effect in the context of pion condensation. Similar effects could then be expected for the inhomogeneous chiral transition.

We now consider flavor-singlet quark matter for a given density and temperature near the transition point. Integrating out the quark degrees of freedom, one can obtain an effective action $S_{\rm eff}$ in terms

[1] A self-consistent solution for inhomogeneous condensates has been analytically discovered in 1+1 dimensions [5,6].

[2] There are also efforts allowing, e.g., strangeness [20] and isospin differences both with [21,22] and without [23–25] charged "pion" condensates.

of the composite fields $\phi_a$, respecting the symmetry $SU(2)_L \times SU(2)_R \simeq O(4)$ in the chiral limit: $S_{\rm eff} \sim \int d^4x \left[ (1/2!)\Gamma^{(2)}\phi_a^2 + (1/4!)\Gamma^{(4)}\left(\phi_a^2\right)^2 + \cdots \right]$. In the following, we call $\Gamma^{(n)}$ the $n$th-order vertex function. Note that $\Gamma^{(2)}$ is closely connected to the inverse of the propagator of the composite fields, $G^{-1}(q_0, \mathbf{q})$, which can be written as $G^{-1}(q_0, \mathbf{q}) = q^2 - m^2 - \Pi_\phi(q_0, \mathbf{q})$, where $m$ is the mass for $\phi_a$ in the vacuum and $\Pi_\phi(q_0, \mathbf{q})$ is the self-energy from the quark particle–hole excitations. In the vicinity of the inhomogeneous chiral transition, $G^{-1}(q_0, \mathbf{q})$ should have a minimum at a nonzero momentum $|\mathbf{q}| = q_c$, reflecting the extent of the spatial modulation in the inhomogeneous chiral phase, and thus can be expanded around $q_c$ as $G^{-1}(q_0, \mathbf{q}) \sim q_0^2 - \gamma\left(|\mathbf{q}|^2 - q_c^2\right)^2 + \text{const.}$ Here one should keep in mind that such a minimum of $G^{-1}(q_0, \mathbf{q})$ gives rise to the singular effect through the loop integrals of the fluctuation fields.

The thermodynamic potential $\Omega$ can be schematically written in a similar form, in terms of the order parameters $\Phi$,

$$\Omega = \int d^3x \left[ \frac{1}{2!}\bar{\Gamma}^{(2)}|\Phi|^2 + \frac{1}{4!}\bar{\Gamma}^{(4)}|\Phi|^4 + \cdots \right], \tag{1}$$

where the coefficients $\bar{\Gamma}^{(n)}$ are modified by the chiral pair fluctuations from $\Gamma^{(n)}$ corresponding to the mean-field approximation (MFA). Indeed, it has been argued [42] that at zero temperature the pion fluctuations alter the order of the phase transition by way of the sign change of the fourth-order vertex function $\bar{\Gamma}^{(4)}$, while the effect of $\bar{\Gamma}^{(2)}$ is discarded. A similar effect has been found [38] in the study of the effects of thermal fluctuations on $\bar{\Gamma}^{(2)}$ and $\bar{\Gamma}^{(4)}$, but the effect of quantum fluctuations is discarded. Therefore, there is no study that simultaneously treats both thermal and quantum fluctuations. In addition, it is unclear how both fluctuations affect the vertexes $\bar{\Gamma}^{(2)}$ and $\bar{\Gamma}^{(4)}$. In this paper, we discuss distinctive features of the inhomogeneous chiral phase transition between the chiral-restored phase and the inhomogeneous chiral phase, along the lines in Refs. [38,42].

The paper is organized as follows. In the next section, we construct a fundamental framework for analyzing the effect of the fluctuations. Also, we extend the Brazovskii theory and show the function form of the thermodynamic potential including the fluctuation effects. In Sect. 3, we present our results for the phase structure between the inhomogeneous chiral and the chiral-restored phase, along with some discussions. Finally, Sect. 4 is devoted to a summary and concluding remarks.

## 2. Effective thermodynamic potential for inhomogeneous condensates

Let us start with the following Lagrangian density in the two-flavor Nambu–Jona-Lasinio (NJL) model [43]:

$$\mathcal{L}_{\rm NJL} = \bar{\psi} i \partial\!\!\!/ \psi + G\left[ \left(\bar{\psi}\psi\right)^2 + \left(\bar{\psi} i\gamma_5 \tau_i \psi\right)^2 \right], \tag{2}$$

where $\psi$ is the quark field, $\tau_i$ denotes the isospin Pauli matrices, and $G$ is a coupling constant of four-Fermi interactions. We employ the MFA, allowing the space-dependent nonzero expectation values for the scalar and pseudoscalar condensates. For later convenience, we introduce the composite fields, $\phi_0 = -2G\bar{\psi}\psi$ and $\phi_i = -2G\bar{\psi}\gamma_5\tau_i\psi$, and the following spatially modulated order parameter:

$$\Phi(z) \equiv -2G\left(\left\langle\bar{\psi}\psi\right\rangle + i\left\langle\bar{\psi} i\gamma_5\tau_3\psi\right\rangle\right) = \Delta(z)e^{i\theta(z)}. \tag{3}$$

Under the calculation within the MFA, the resulting inhomogeneous chiral phase has two boundaries [4,7]: one is the onset boundary between the homogeneous and the inhomogeneous chiral phase, the other is the termination boundary between the inhomogeneous chiral and the chiral-restored phase. The former is of the first order for the DCDW condensate and of the second order for the RKC condensate within the MFA. The latter, on the other hand, is always of the second order for both cases. In the following, we concentrate on the termination boundary.

### 2.1. *Propagator of the composite fields*

In this paper, we are interested in the inhomogeneous chiral phase prescribed by Eq. (3). In order to discuss the order change of the phase transition, we only construct the thermodynamic potential near the phase boundary and focus on it at least up to the fourth order in powers of $\Phi(z)$. We start from an effective action in the chiral-restored phase. The effective action can be deduced from QCD, but one may derive it as well by using the effective model of QCD, e.g., the NJL model.

Integrating out the quark degrees of freedom, one can obtain the following thermal effective action, with the Matsubara frequency $\omega_n = 2n\pi T$,

$$S_0(\phi) = \frac{1}{2!}T\sum_{n_1}\int\frac{d^3q_1}{(2\pi)^3}\Gamma^{(2)}_{\rm ps}(\omega_{n_1},\mathbf{q_1})\,\phi(\omega_{n_1},\mathbf{q_1})\,\phi(-\omega_{n_1},-\mathbf{q_1}) + \frac{1}{4!}T^4\prod_{i=1}^{4}\sum_{n_i}\int\frac{d^3q_i}{(2\pi)^3}\hat{\lambda}\left(\{\omega_{n_i}\},\{\mathbf{q_i}\}\right)\phi(\omega_{n_1},\mathbf{q_1})\,\phi(\omega_{n_2},\mathbf{q_2})\,\phi(\omega_{n_3},\mathbf{q_3})\,\phi(\omega_{n_4},\mathbf{q_4}). \tag{4}$$

Here, the odd-power terms of $\phi$ should vanish due to the chiral symmetry. Note that while the effective action should be written in a symmetric form for all composite fields $\phi_a$, it is sufficient to keep only the specific composite field $\phi_0$ or $\phi_3$.[3] Hereafter we only take $\phi \equiv \phi_3 = -2G\bar{\psi}i\gamma_5\tau_3\psi$ to discuss the inhomogeneous chiral transition, especially for the DCDW. The coefficients of each order of $\phi$ in the action should be determined from the underlying quark dynamics. Here, the coefficient $\hat{\lambda}\left(\{\omega_{n_i}\},\{\mathbf{q_i}\}\right) = \hat{\lambda}(\omega_1,\omega_2,\omega_3,\omega_4,\mathbf{q_1},\mathbf{q_2},\mathbf{q_3},\mathbf{q_4})$ denotes the interaction vertex among $\phi$.

In the following, we derive the formula of $\Gamma^{(2)}_{\rm ps}(\omega_n,\mathbf{q})$. We now simply evaluate $\Gamma^{(2)}_{\rm ps}(\omega_n,\mathbf{q})$ within the random phase approximation (RPA) in the NJL model [44], instead of the full calculation. By introducing the $q\bar{q}$ polarization function $\Pi^0_{\rm ps}(\omega_n,\mathbf{q})$, we find

$$\Gamma^{(2)}_{\rm ps}(\omega_n,\mathbf{q}) = \frac{1-2G\Pi^0_{\rm ps}(\omega_n,\mathbf{q})}{2G}. \tag{5}$$

Here, $\Pi^0_{\rm ps}(\omega_n,\mathbf{q})$ is given by

$$\begin{aligned}\Pi^0_{\rm ps}(\omega_n,\mathbf{q}) &\equiv T\sum_m\int\frac{d^3p}{(2\pi)^3}{\rm tr}\left[i\gamma_5\tau_3 S_\beta(\omega_n+\tilde{\omega}_m,\mathbf{q}+\mathbf{p})\,i\gamma_5\tau_3 S_\beta(\tilde{\omega}_m,\mathbf{p})\right]\\ &= \Pi^{0,{\rm vac}}_{\rm ps}(\omega_n,\mathbf{q}) + \Pi^{0,{\rm med}}_{\rm ps}(\omega_n,\mathbf{q}),\end{aligned} \tag{6}$$

where $\tilde{\omega}_m = (2m+1)\pi T$ $(m\in\mathbb{Z})$ is the Matsubara frequency for quark in the loop integral [45], $S_\beta(\tilde{\omega}_m,\mathbf{p})$ is the thermal quark propagator, and $\Pi^{0,{\rm vac}}_{\rm ps}(\omega_n,\mathbf{q})$ and $\Pi^{0,{\rm med}}_{\rm ps}(\omega_n,\mathbf{q})$ are the vacuum and the thermal contributions to the polarization function, respectively. Employing a straightforward calculation, we obtain

$$\Pi^{0,{\rm vac}}_{\rm ps}(\omega_n,\mathbf{q}) = \frac{N_f N_c}{(2\pi)^2}\left[\Lambda^2 - \frac{\omega_n^2+|\mathbf{q}|^2}{2}\int_0^1 dt\int_{1/\Lambda^2}^{\infty}\frac{d\tau}{\tau}e^{-(\omega_n^2+|\mathbf{q}|^2)t(1-t)\tau}\right], \tag{7}$$

[3] Other composite fields also contribute to the thermodynamic potential, but their coupling with the condensate is suppressed by $O(N^{-1})$ with the number of $\phi_a$, $N$, relative to $\phi_0$ or $\phi_3$, once the specific form of $\Phi$ is assigned.

and

$$\Pi_{\rm ps}^{0,{\rm med}}(\omega_n,\mathbf{q}) = -\frac{2N_f N_c}{(2\pi)^2}\sum_{s=\pm}\int_0^\infty pdp\,\frac{1}{e^{\beta(p+s\mu)}+1}\left(2+\frac{\omega_n^2+|\mathbf{q}|^2}{4p\,|\mathbf{q}|}\log\left|\frac{\omega_n^2+(|\mathbf{q}|-2p)^2}{\omega_n^2+(|\mathbf{q}|+2p)^2}\right|\right), \tag{8}$$

where we have used the proper time regularization (PTR) in $\Pi_{\rm ps}^{0,{\rm vac}}(\omega_n,\mathbf{q})$. For details, see Appendix A.

In the following, we derive the formula for the imaginary-time propagator of the composite field. Note here that $1-2G\Pi_{\rm ps}^{0,{\rm vac}}$ is associated with the propagator of the composite field in the vacuum,

$$\begin{aligned}1-2G\Pi_{\rm ps}^{0,{\rm vac}}(\omega_n,\mathbf{q}) &\sim 1-2G\Pi_{\rm ps}^{0,{\rm vac}}(0,\mathbf{0})+2G\frac{\partial}{\partial q^2}\Pi_{\rm ps}^{0,{\rm vac}}\Big|_{\omega_n=|\mathbf{q}|=0}\left(\omega_n^2+|\mathbf{q}|^2\right)\\ &= 2Gg_{\phi qq}^{-2}G_{\rm ps,vac}^{-1}(\omega_n,\mathbf{q}),\end{aligned} \tag{9}$$

where $G_{\rm ps,vac}(\omega_n,\mathbf{q}) = \left[m^2+\omega_n^2+|\mathbf{q}|^2\right]^{-1}$ is the imaginary-time propagator of the composite field, $m^2 \equiv g_{\phi qq}^2\left(1-2G\Pi_{\rm ps}^{0,{\rm vac}}(0,\ \mathbf{0})\right)/2G$ is the mass term for $\phi$, and $g_{\phi qq}$ is the effective coupling constant between $\phi$ and quarks defined by $\partial\Pi_{\rm ps}^{0,{\rm vac}}/\partial q^2|_{q^2=0} = g_{\phi qq}^{-2}$ [46]. We remark that there is the dynamically generated kinetic term for the composite field made of $q\bar{q}$ by way of the vacuum polarization, while it does not apparently exist in the NJL model [47,48]. Thus, $\Gamma_{\rm ps}^{(2)}$ can be written as

$$\left[\Gamma_{\rm ps}^{(2)}(\omega_n,\mathbf{q})\right]^{-1} \sim \frac{g_{\phi qq}^2}{m^2+\omega_n^2+|\mathbf{q}|^2-g_{\phi qq}^2\Pi_{\rm ps}^{0,{\rm med}}(\omega_n,\mathbf{q})} \equiv g_{\phi qq}^2 G_{\rm ps}(\omega_n,\mathbf{q}), \tag{10}$$

where $G_{\rm ps}(\omega_n,\mathbf{q})$ is the propagator in medium and $\Pi_{\rm ps}^{0,{\rm med}}(\omega_n,\ \mathbf{q})$ represents the self-energy coming from the interaction with the surrounding quarks.

We should keep in mind that the field variable $\phi$ in Eq. (4) should be properly rescaled because $\Gamma_{\rm ps}^{(2)}$ does not actually render a form of the inverse propagator. In order to extract the physical results, we rewrite the action in terms of the rescaled field variable $\tilde{\phi} \equiv g_{\phi qq}\phi$. Thus, the coefficients in Eq. (4) are rewritten as follows: $\Gamma_{\rm ps}^{(2)} \to G_{\rm ps}^{-1}$ and $\hat{\lambda} \to \tilde{\lambda} \equiv g_{\phi qq}^{-4}\hat{\lambda}$. Consequently, the physical action has the same form as the original one, while the coefficients are modified. For simplicity, we write again $\tilde{\phi}$ and $\tilde{\lambda}$ as $\phi$ and $\hat{\lambda}$, respectively.

In the static limit ($\omega_n = 0$), $G_{\rm ps}(0,\mathbf{q})$ is proportional to the correlation function of the pseudoscalar density or the static susceptibility in the pseudoscalar channel; when the static susceptibility diverges at a finite momentum, it is a signal of the second-order phase transition to the inhomogeneous chiral phase [4]. This method is called the correlation function method (for details, see Appendix B). Note that $G_{\rm ps}^{-1}(0,\ \mathbf{q})$ has a minimum with finite $|\ \mathbf{q}|$ near the transition point.[4] Since $G_{\rm ps}^{-1}(0,\mathbf{q})$ is an even function of $|\mathbf{q}|$ [see Eq. (B1) in Appendix B], we can expand it as follows:

$$G_{\rm ps}^{-1}(0,\mathbf{q}) \sim \tau+\gamma\left(|\mathbf{q}|^2-q_c^2\right)^2, \tag{11}$$

where $q_c$ is defined as the minimum point of $G_{\rm ps}^{-1}(0,\mathbf{q})$, $\partial_q\Pi_{\rm ps}^0(0,\mathbf{q_c}) = 0$ (for a numerical confirmation, see Fig. B1). The presence of the minimum in $G_{\rm ps}^{-1}(0,\mathbf{q})$ with finite momentum is physically

[4] For the homogeneous chiral transition, it has a minimum with $|\ \mathbf{q}| = 0$ [see Eq. (36)].

interpreted as the consequence of the derivative coupling between the $q\bar{q}$ polarization and quarks in the pseudoscalar channel. The quantities $\tau$ and $\gamma$ are defined as

$$\tau \equiv G_{\rm ps}^{-1}(0,\mathbf{q})|_{|\mathbf{q}|=q_c} = m^2 - g_{\phi qq}^2 \Pi_{\rm ps}^{0,\rm med}(0,\mathbf{q})|_{|\mathbf{q}|=q_c}, \tag{12}$$

and

$$\gamma \equiv \frac{1}{2}\frac{d^2}{(d|\mathbf{q}|^2)^2} G_{\rm ps}^{-1}(0,\mathbf{q})\bigg|_{|\mathbf{q}|=q_c} = -\frac{g_{\phi qq}^2}{2}\frac{d^2}{(d|\mathbf{q}|^2)^2}\Pi_{\rm ps}^{0,\rm med}(0,\mathbf{q})\bigg|_{|\mathbf{q}|=q_c}, \tag{13}$$

respectively, which are functions of temperature and chemical potential.

If we consider the chiral pair fluctuations around the condensate, we should take into account the loop diagrams composed of the propagator, where the summation over the Matsubara frequency is needed. Thus, we consider the propagator with the external Matsubara frequency: $g_{\phi qq}^2 G_{\rm ps}(\omega_n,\mathbf{q}) = 2G/(1-2G\Pi_{\rm ps}^0(\omega_n,\mathbf{q}))$. Here, $G_{\rm ps}^{-1}(\omega_n,\mathbf{q})$ is expanded in the same way as Eq. (11),

$$G_{\rm ps}^{-1}(\omega_n,\mathbf{q}) \sim \tau + \gamma\left(|\mathbf{q}|^2 - q_c^2\right)^2 + f(\omega_n,\mathbf{q}), \tag{14}$$

where $f(\omega_n,\mathbf{q}) = \omega_n^2 - g_{\phi qq}^2\left(\Pi_{\rm ps}^{0,\rm med}(\omega_n,\mathbf{q}) - \Pi_{\rm ps}^{0,\rm med}(0,\mathbf{q})\right)$ satisfies $f(0,\mathbf{q}) = 0$. When we evaluate the loop diagrams of $G_{\rm ps}(\omega_n,\mathbf{q})$ in the numerical calculation, we further approximate $f(\omega_n,\mathbf{q})$ in Eq. (14) by expanding it up to the second order in powers of $\omega_n$ without loss of essentials: $f(\omega_n,\mathbf{q}) \sim a_1(|\mathbf{q}|)\,|\omega_n| + a_2(|\mathbf{q}|)\omega_n^2$. Since the momentum around $q_c$ mainly contributes to the loop integrals of $G_{\rm ps}$, we here approximate $a_i(|\mathbf{q}|)$ by $a_i(q_c) \equiv a_i$.

The resulting formula of the propagator reads

$$G_{\rm ps}^{-1}(\omega_n,\mathbf{q}) \sim \tau + \gamma\left(|\mathbf{q}|^2 - q_c^2\right)^2 + a_1\,|\omega_n| + a_2\omega_n^2, \tag{15}$$

where

$$a_1 \equiv \frac{d}{dx} G_{\rm ps}^{-1}(x,\mathbf{q})\bigg|_{x=0,|\mathbf{q}|=q_c} = -g_{\phi qq}^2\frac{d}{dx}\Pi_{\rm ps}^{0,\rm med}(x,\mathbf{q})\bigg|_{x=0,|\mathbf{q}|=q_c}, \tag{16}$$

and

$$a_2 \equiv \frac{1}{2}\frac{d^2}{dx^2} G_{\rm ps}^{-1}(x,\mathbf{q})\bigg|_{x=0,|\mathbf{q}|=q_c} = 1 - \frac{1}{2}\frac{d^2}{dx^2}\Pi_{\rm ps}^{0,\rm med}(x,\mathbf{q})\bigg|_{x=0,|\mathbf{q}|=q_c}. \tag{17}$$

### 2.2. *Thermodynamic potential*

Now we are going to construct the effective thermodynamic potential, starting with the effective action in Eq. (4).

In the beginning, we show the formula of $\hat{\lambda}(\{\omega_{n_i}\},\{\mathbf{q_i}\})$. Generally the coupling function $\hat{\lambda}(\{\omega_{n_i}\},\{\mathbf{q_i}\})$ should be nonlocal and depends on $\{\omega_{n_i}\}$ and $\{\mathbf{q_i}\}$. In the following we approximate it as a local four-point function: $\hat{\lambda}(\{\omega_{n_i}\},\{\mathbf{q_i}\}) \sim \lambda\delta(\mathbf{q_1}+\mathbf{q_2}+\mathbf{q_3}+\mathbf{q_4})$ with the coupling constant $\lambda$. The proper formula of $\lambda$ can be obtained by the one-loop quark propagator,

$$\lambda \sim T\sum_m \int \frac{d^3p}{(2\pi)^3}\mathrm{tr}\Big[ i\gamma_5\tau_3 S_\beta(\tilde{\omega}_m,\mathbf{p}+\mathbf{q_c})\, i\gamma_5\tau_3 S_\beta(\tilde{\omega}_m,\mathbf{p}) \times i\gamma_5\tau_3 S_\beta(\tilde{\omega}_m,\mathbf{p}-\mathbf{q_c})\, i\gamma_5\tau_3 S_\beta(\tilde{\omega}_m,\mathbf{p})\Big], \tag{18}$$

because $|\mathbf{q}| \sim q_c$ of the propagator predominantly contributes to the loop diagrams of the propagator. A similar discussion is given in the context of pion condensation [49].

We here divide the composite field into the thermal average $\Phi = \langle\phi\rangle$ and the fluctuation field $\xi$: $\phi(\omega_n, \mathbf{q}) = \beta\Phi(\mathbf{q})\delta_{n0} + \xi(\omega_n, \mathbf{q})$. Since the fluctuation field $\xi$ depends not only on the momentum but on the Matsubara frequency, the quantum and thermal fluctuations are properly taken into account in the finite temperature and chemical potential region.

The effective action is then divided into two components: $S_0(\phi) = S_0(\beta\Phi\delta_{n0}) + S_1(\Phi, \xi)$, where

$$\begin{aligned}
S_1(\Phi,\xi) = &\int \frac{d^3p_1}{(2\pi)^3} G_{\rm ps}^{-1}(0,\mathbf{p_1})\,\Phi(\mathbf{p_1})\xi(0,-\mathbf{p_1}) \\
&+ \frac{1}{2}T\sum_{n_1}\int \frac{d^3p_1}{(2\pi)^3} G_{\rm ps}^{-1}(\omega_{n_1},\mathbf{p_1})\,\xi(\omega_{n_1},\mathbf{p_1})\xi(-\omega_{n_1},-\mathbf{p_1}) \\
&+ \frac{\lambda}{6}\prod_{i=1}^{3}\int \frac{d^3p_i}{(2\pi)^3}\Phi(\mathbf{p_1})\Phi(\mathbf{p_2})\Phi(\mathbf{p_3})\xi(0,-\mathbf{p_1}-\mathbf{p_2}-\mathbf{p_3}) \\
&+ \frac{\lambda}{4}T\sum_{n_3}\prod_{i=1}^{3}\int \frac{d^3p_i}{(2\pi)^3}\Phi(\mathbf{p_1})\Phi(\mathbf{p_2})\xi(\omega_{n_3},\mathbf{p_3})\xi(-\omega_{n_3},-\mathbf{p_1}-\mathbf{p_2}-\mathbf{p_3}) \\
&+ \frac{\lambda}{6}T^2\sum_{n_2,n_3}\prod_{i=1}^{3}\int \frac{d^3p_i}{(2\pi)^3}\Phi(\mathbf{p_1})\xi(\omega_{n_2},\mathbf{p_2})\xi(\omega_{n_3},\mathbf{p_3})\xi(-\omega_{n_2}-\omega_{n_3},-\mathbf{p_1}-\mathbf{p_2}-\mathbf{p_3}) \\
&+ \frac{\lambda}{24}T^3\prod_{i=1}^{3}\sum_{n_i}\int \frac{d^3p_i}{(2\pi)^3}\xi(\omega_{n_1},\mathbf{p_1})\xi(\omega_{n_2},\mathbf{p_2})\xi(\omega_{n_3},\mathbf{p_3}) \\
&\times\xi(-\omega_{n_1}-\omega_{n_2}-\omega_{n_3},-\mathbf{p_1}-\mathbf{p_2}-\mathbf{p_3}). \qquad (19)
\end{aligned}$$

Here, $S_0$ has already been given in Eq. (4). Before deriving the vertex functions of the order parameter $\bar{\Gamma}^{(n)}$ in the thermodynamic potential, we remark on $S_1(\Phi, \xi)$. The first term in Eq. (19) corresponds to the leading contribution to the tadpole diagram. The second and fourth terms contribute to the propagator of $\xi$ in the presence of the condensate. The third and fifth terms represent the couplings of $\xi$ with the condensate. Finally, the sixth term represents the contact four-point interaction among $\xi$, which would mainly contribute to the self-energy of $\xi$.

Employing the functional integral with $\xi$, we obtain the following effective thermodynamic potential:

$$\Omega(\Phi) = TS_0(\beta\Phi\delta_{n0}) - T\log\int\mathcal{D}\xi\ \exp\{-S_1(\Phi,\xi)\}. \qquad (20)$$

If we neglect the effect of the fluctuations given by the second term in Eq. (20), the thermodynamic potential coincides with that within the MFA. Expanding Eq. (20) with respect to the order parameter, we find

$$\begin{aligned}
\Omega(\Phi) = &\frac{1}{2!}\int\frac{d^3p_1\,d^3p_2}{(2\pi)^6}\bar{\Gamma}^{(2)}(\mathbf{p_1},\mathbf{p_2})\,\Phi(-\mathbf{p_1})\,\Phi(-\mathbf{p_2}) + \frac{1}{4!}\int\frac{d^3p_1\,d^3p_2d^3p_3d^3p_4}{(2\pi)^{12}} \\
&\times\bar{\Gamma}^{(4)}(\mathbf{p_1},\mathbf{p_2},\mathbf{p_3},\mathbf{p_4})\,\Phi(-\mathbf{p_1})\,\Phi(-\mathbf{p_2})\,\Phi(-\mathbf{p_3})\,\Phi(-\mathbf{p_4})\cdots. \qquad (21)
\end{aligned}$$

In the following, we derive the modified vertex functions for the effective thermodynamic potential, which are defined as

$$\bar{\Gamma}^{(n)}(\mathbf{q_1},\mathbf{q_2},\ldots,\mathbf{q_n}) = \left.\frac{\delta^n\Omega}{\delta\Phi(-\mathbf{q}_1)\delta\Phi(-\mathbf{q}_2)\cdots\delta\Phi(-\mathbf{q}_n)}\right|_{\Phi=0}. \qquad (22)$$

We then obtain the first-order functional derivative of $\Omega$, which is a key equation for deriving the higher-order modified vertex functions:

$$\begin{aligned}\frac{\delta\Omega}{\delta\Phi(-\mathbf{q_1})} &= G_{\rm ps}^{-1}(0,\mathbf{q_1})\,\Phi(\mathbf{q_1}) + \frac{\lambda}{3!}\int\frac{d^3p_2\,d^3p_3}{(2\pi)^6}\Phi(\mathbf{p_2})\,\Phi(\mathbf{p_3})\,\Phi(\mathbf{q_1}-\mathbf{p_2}-\mathbf{p_3})\\ &+\frac{\lambda}{2!}T^2\sum_n\int\frac{d^3p_2\,d^3p_3}{(2\pi)^6}\langle\xi(\omega_n,\mathbf{p_2})\,\xi(-\omega_n,-\mathbf{p_3})\rangle_\xi\,\Phi(\mathbf{q_1}-\mathbf{p_2}-\mathbf{p_3})\\ &+\frac{\lambda}{3!}T^3\sum_{n_2,n_3}\int\frac{d^3p_2\,d^3p_3}{(2\pi)^6}\left\langle\xi(\omega_{n_2},\mathbf{p_2})\,\xi(\omega_{n_3},\mathbf{p_3})\,\xi(-\omega_{n_2}-\omega_{n_3},\mathbf{q_1}-\mathbf{q_2}-\mathbf{p_3})\right\rangle_\xi,\end{aligned} \tag{23}$$

where the symbol $\langle\cdots\rangle_\xi$ denotes the thermal average. Solving the equation $\delta\Omega\delta\Phi(-\mathbf{q_1})=0$, we obtain possible solutions of the order parameter. Also, these solutions admit that the thermodynamic potential can be written as a function of amplitude ($\Delta$) and wave vector ($\mathbf{q}$) at each temperature and chemical potential. Note here that $\Delta=0$ is the trivial solution and gives the minimum of the thermodynamic potential in the chiral-restored phase. The phase transition should occur with the wave vector, $\mathbf{q}\sim\mathbf{q_c}$, which minimizes the curvature of the thermodynamic potential near $\Delta=0$. Thus, we can expect that $\Phi(\mathbf{q})\sim\Phi(\pm\mathbf{q_c})$ plays the primary role near the critical point.

In the following we evaluate the thermal average $\langle\xi(\omega_n,\mathbf{p_2})\xi(-\omega_n,-\mathbf{p_3})\rangle_\xi$. In general, the propagator of $\xi$ does not preserve its momentum between the in and out states because of the presence of the fourth term in Eq. (19). However, we can neglect the off-diagonal momentum component ($\mathbf{p_2}\neq\mathbf{p_3}$) in $\langle\xi(\omega_n,\mathbf{p_2})\,\xi(-\omega_n,-\mathbf{p_3})\rangle_\xi$, as long as we consider the loop diagrams of the propagator [38]; since $\langle\xi(\omega_n,\mathbf{p_2})\,\xi(-\omega_n,-\mathbf{p_3})\rangle_\xi=\beta\delta(\mathbf{p_2}-\mathbf{p_3})\,G_{\rm ps}(\omega_n,\mathbf{p}_2)$ in the lowest order of $\lambda$ and $|\mathbf{p}_2|\sim q_c$ give a singular contribution in the loop integrals, the diagonal momentum components always dominate over the off-diagonal ones in higher-order diagrams.

If we consider the correction to the self-energy, the lowest-order diagram is a simple loop and gives $T\sum_n\int d^3p/(2\pi)^3G_{\rm ps}(\omega_n,\mathbf{p})$. Since the simple loop integral exhibits a singular behavior $\sim1/\sqrt{r}$, we must resum the higher-order diagrams connecting the simple loops by the sixth term in Eq. (19) to get a meaningful result. Employing the Dyson–Schwinger equation depicted in Fig. 1, we obtain the modified propagator of $\xi$,

$$\left\langle\xi(\omega_n,\mathbf{q_1})\,\xi(-\omega_n,-\mathbf{q_2})\right\rangle_\xi=\frac{\beta\delta(\mathbf{q_1}-\mathbf{q_2})}{r+\gamma\left(|\mathbf{q_1}|^2-q_c^2\right)^2+a_1|\omega_n|+a_2\omega_n^2}, \tag{24}$$

where $r$ is the modified mass term of the propagator, satisfying the equation

$$\begin{aligned}r&=\tau+V^{-1}\frac{\lambda}{2}\int\frac{d^3p}{(2\pi)^3}\Phi(\mathbf{p})\,\Phi(-\mathbf{p})\\ &+\frac{\lambda}{2}T\sum_n\int\frac{d^3p}{(2\pi)^3}\frac{1}{r+\gamma\left(|\mathbf{p}|^2-q_c^2\right)^2+a_1\,|\omega_n|+a_2\omega_n^2}.\end{aligned} \tag{25}$$

Here, $V$ is the volume of the system. Note that Fig. 1 shows a part of the self-energy diagrams.

We have discarded part of the tadpole diagrams coming from the third term in Eq. (19) and higher-order diagrams (see, e.g., Fig. 2). The left diagram in Fig. 2 arises from the fourth term in Eq. (23), and predominantly contributes at high temperatures, so that further studies are needed to determine the phase boundary near the Lifshitz point (LP) where the homogeneous chiral, inhomogeneous chiral, and chiral-restored phases meet. Accordingly, we, hereafter, discard the fourth term in Eq. (23). The right diagram in Fig. 2 is less important than the second diagram in Fig. 1 by at least $\mathcal{O}(\lambda)$.

**Fig. 1.** Dyson–Schwinger equation for the self-energy. The single (double) line corresponds to the tree-level (renormalized) propagator of $\xi$.

**Fig. 2.** Next-to-leading-order diagrams contributing to the Dyson–Schwinger equation.

From Eqs. (24) and (25), we can rewrite Eq. (23) as

$$\frac{\delta\Omega}{\delta\Phi(-\mathbf{q_1})} = \left[r + \gamma\left(|\mathbf{q_1}|^2 - q_c^2\right)^2\right]\Phi(\mathbf{q_1}) - V^{-1}\frac{\lambda}{2!}\Phi(\mathbf{q_1})\int\frac{d^3p_2}{(2\pi)^3}\Phi(\mathbf{p_2})\,\Phi(-\mathbf{p_2}) + \frac{\lambda}{3!}\sum_n\int\frac{d^3p_2\,d^3p_3}{(2\pi)^6}\Phi(\mathbf{p_2})\,\Phi(\mathbf{p_3})\,\Phi(\mathbf{q_1}-\mathbf{p_2}-\mathbf{p_3})\,. \tag{26}$$

Subsequent functional derivatives to Eq. (26) give the formula of any order of modified vertex functions. Since any odd-order term is equal to zero, we hereafter consider only the even-order terms.

In the following, we derive the second- and fourth-order modified vertex functions. We first show the formula of the second-order vertex function. Performing functional derivative to Eq. (26), the formula of $\bar{\Gamma}^{(2)}$ is given by

$$\bar{\Gamma}^{(2)}(\mathbf{q_1},\mathbf{q_2}) = \delta(\mathbf{q_1}+\mathbf{q_2})\left[\tau_R + \gamma\left(|\mathbf{q_1}|^2 - q_c^2\right)^2\right], \tag{27}$$

where $\tau_R \equiv r|_{\Phi=0}$ is the modified mass term of $\phi$ and satisfies the equation

$$\tau = \tau_R - \frac{\lambda}{2}T\sum_n\int\frac{d^3p}{(2\pi)^3}\,G^R_{\rm ps}(\omega_n,\mathbf{p}), \tag{28}$$

where $G^R_{\rm ps}(\omega_n,\mathbf{p}) = 1/[\tau_R + \gamma\left(|\mathbf{p}|^2 - q_c^2\right)^2 + a_1\,|\omega_n| + a_2\omega_n^2]$. The second term in Eq. (28) represents the contribution of the self-energy corresponding to the second diagram in Fig. 1. We can analytically perform the Matsubara frequency sum as

$$\tau = \tau_R + \frac{\lambda}{8a_2\pi^3}\int_0^\infty dp\int_{1/\Lambda^2}^\infty\frac{dx}{x}\,\frac{p^2}{\rho}\left(e^{-(\sigma-\rho)^2x^2} - e^{-(\sigma+\rho)^2x^2}\right) - \frac{\lambda}{16\pi}\,\frac{q_cT}{\sqrt{\gamma}}\,\frac{1}{\sqrt{\tau_R}} - \frac{\lambda\sigma}{a_2\pi^3}\int_0^\infty dp\int_0^\infty dz\,\frac{1}{e^{z/T}+1}\,\frac{p^2z}{\left[z^2+(\sigma+\rho)^2\right]\left[z^2+(\sigma-\rho)^2\right]}. \tag{29}$$

Here, the second term is the vacuum contribution, the third term comes from the lowest order of the Matsubara frequency, and the fourth term is the residual thermal contribution. The vacuum contribution has been regularized with the help of the PTR scheme, and $\sigma$ and $\rho$ are defined by $\sigma = -\frac{a_1}{2a_2} - \pi T$ and $\rho = \sqrt{a_1^2 - 4a_2\eta}/2a_2$ with $\eta \equiv \tau_R + \gamma\left(|\mathbf{p}|^2 - q_c^2\right)^2$, respectively (for details, see Appendix C). The above equation shows a singular behavior of $\tau_R$. Here, the second and third terms diverge at $\tau_R \to 0$ (see Fig. 6 for the divergence of the second term), so that $\tau_R$ is positive definite, while $\tau$ becomes negative at any point of the inhomogeneous chiral phase within the MFA. Thus, the second-order phase transition is prohibited by the chiral pair fluctuations (cf. Refs. [50–52]).


**Fig. 3.** Two-$\phi$ exchange diagram $L(\mathbf{k})$. The double line denotes $G^R_{\rm ps}(\omega_n, \mathbf{p})$.

Next we present the formula of the fourth-order vertex function. From Eq. (26), as in the second-order vertex function, we find

$$\bar{\Gamma}^{(4)}(\mathbf{q_1}, \mathbf{q_2}, \mathbf{q_3}, \mathbf{q_4}) = \lambda\delta(\mathbf{q_1}+\mathbf{q_2}+\mathbf{q_3}+\mathbf{q_4}) + V^{-1}\lambda\frac{-\frac{\lambda}{2}L(0)}{1+\frac{\lambda}{2}L(0)}\big(\delta(\mathbf{q_1}+\mathbf{q_2})\,\delta(\mathbf{q_3}+\mathbf{q_4}) + \delta(\mathbf{q_1}+\mathbf{q_3})\,\delta(\mathbf{q_2}+\mathbf{q_4}) + \delta(\mathbf{q_1}+\mathbf{q_4})\,\delta(\mathbf{q_2}+\mathbf{q_3})\big), \tag{30}$$

where $L(\mathbf{k})$ represents the two-$\phi$ exchange diagram between the four-point vertexes depicted in Fig. 3 and is given by

$$L(\mathbf{k}) = T\sum_n \int \frac{d^3p}{(2\pi)^3}\, G^R_{\rm ps}(\omega_n, \mathbf{p}) G^R_{\rm ps}(-\omega_n, \mathbf{k}-\mathbf{p}). \tag{31}$$

The first term in Eq. (30) is obtained by performing functional derivatives to the third term in Eq. (26). The second term in Eq. (30) is obtained by the first and second terms in Eq. (26). The resummation of the two-$\phi$ exchange diagram is obtained by performing the functional derivatives to the self-energy of $r$ given by the second term in Fig. 1. Note that this is a dangerous diagram and has been shown to exhibit a singular behavior [42]; in the limit $k \to 0$, $L(0)$ will diverge near the transition point, $\tau_R = 0$. Thus, we find

$$\begin{aligned} L(0) &= \frac{1}{16\pi}\frac{q_c}{\sqrt{\gamma}}\left(\frac{1}{\pi a_1}\frac{1}{\sqrt{\tau_R+\pi T a_1}} + \frac{T}{\tau_R^{3/2}}\right) \\ &\quad - \frac{2}{\pi^3}a_1\int_0^\infty dp\int_0^\infty dz\,\frac{1}{e^{z/T}+1}\,\frac{\left(\tau_R+\gamma\left(p^2-q_c^2\right)^2+\pi T a_1\right)^2 p^2 z}{\left[a_1^2 z^2+\left(\tau_R+\gamma\left(p^2-q_c^2\right)^2+\pi T a_1\right)^2\right]^2} \\ &\sim \frac{1}{16\pi}\frac{q_c}{\sqrt{\gamma}}\left(\frac{1}{\pi a_1}\frac{1}{\sqrt{\tau_R}} + \frac{T}{\tau_R^{3/2}}\right), \end{aligned} \tag{32}$$

which surely diverges as $\tau_R \to 0$. In the last line here we have kept the terms which give the leading contribution to $L(0)$.

In order to clearly see the appearance of the fluctuation-induced phase transition, we here rewrite $\bar{\Gamma}^{(4)}$ as a contact interaction. We perform the isotropic approximation [53]: we tune it to make both the nonlocal and local interactions give the same contribution for the $\Phi^4$ term in the thermodynamic potential,

$$\begin{aligned} &\bar{V}^{-1}\big(\delta(\mathbf{q_1}+\mathbf{q_2})\,\delta(\mathbf{q_3}+\mathbf{q_4}) + \delta(\mathbf{q_1}+\mathbf{q_3})\,\delta(\mathbf{q_2}+\mathbf{q_4}) + \delta(\mathbf{q_1}+\mathbf{q_4})\,\delta(\mathbf{q_2}+\mathbf{q_3})\big) \\ &\quad \sim 2\delta(\mathbf{q_1}+\mathbf{q_2}+\mathbf{q_3}+\mathbf{q_4}), \end{aligned} \tag{33}$$

where $\bar{V}$ is the volume of the Wigner–Seitz cell, $\bar{V} = \pi l^2/q$, with $l$ being the system length for $x$ and $y$ directions. The factor 2 is obtained by inserting an explicit form of $\Phi = \Delta\sin(qz)$ as follows. Evaluating the $\Phi^4$ term in the thermodynamic potential from the second term in Eq. (30) with

$\Phi = \Delta \sin(qz)$, we find

$$3 \times \left( \frac{q}{\pi} \int_0^{\pi/q} dz \Phi^2(z) \right)^2 = 2 \times \frac{q}{\pi} \int_0^{\pi/q} dz \Phi^4(z). \tag{34}$$

Here, the factor 3 comes from the combinatorial factor to choose $\Phi^2$ pairs from $\Phi^4$. While we have used a specific form of $\Phi$, we can easily apply this procedure for any form of $\Phi$.

Consequently, we obtain $\bar{\Gamma}^{(4)}$ as a coefficient of $\Phi^4$,

$$\bar{\Gamma}^{(4)} \sim \lambda \frac{1 - \frac{\lambda}{2} L(0)}{1 + \frac{\lambda}{2} L(0)} \delta(\mathbf{q_1} + \mathbf{q_2} + \mathbf{q_3} + \mathbf{q_4}). \tag{35}$$

As we will see in the next section, $\bar{\Gamma}^{(4)}$ is rapidly decreasing just after $\bar{\Gamma}^{(4)} = 0$ (see Fig. 7), and if the curvature of the thermodynamic potential $\Omega(\bar{\Phi})$ at $\bar{\Phi} = 0$, which is equal to $\tau_R$, is sufficiently small near the critical point, $\Omega(\bar{\Phi})$ should touch the level line of $\Omega(0)$ at small $\bar{\Phi}$. Thus, we may say that $\bar{\Gamma}^{(4)} = 0$ is a signal of the first-order phase transition [38,42].

We find from Eq. (32) that our procedure contains both quantum and thermal fluctuations. In fact, the first term in Eq. (32) remains in the limit $T \to 0$, so that the corresponding term exhibits the effect of the quantum fluctuations. This term corresponds to the term derived by Dyugaev [42]. Thus, we find that our formula is more refined. While in the study by Dyugaev only the effect associated with the fourth-order vertex function is taken into account and hence $L(0)$ is proportional to $1/\sqrt{\tau}$, we consider the effect of the fluctuation associated with both the second-order and the fourth-order vertex function in our work. Therefore, $L(0)$ is proportional to $1/\sqrt{\tau_R}$ and its coefficient completely coincides with that derived by Dyugaev. In addition, the term with $T/\tau_R^{3/2}$ in Eq. (32) completely coincides with that in the work by Brazovskii [38]. Thus, our method indeed contains the results of earlier seminal works.

For the fluctuation effect associated with the sixth-order vertex function, it turns out to be negligible from a straightforward calculation. Therefore, unlike $\bar{\Gamma}^{(2)}$ and $\bar{\Gamma}^{(4)}$, there is no influence on the determination of a critical point.

## 3. Phase boundary

### 3.1. Homogeneous case

In order to figure out the difference in the effect of the chiral pair fluctuations between the homogeneous and inhomogeneous chiral transitions, we now discuss the phase boundary in the high temperature and small chemical potential region, where the inhomogeneous chiral phase is thermodynamically disfavored compared to the homogeneous phase. In this paper, we take $\Lambda = 660.37\,\mathrm{MeV}$ and $G\Lambda^2 = 6.35$ so as to reproduce the constituent quark mass and the pion decay constant in the vacuum.

Our framework given in Sect. 2.2 is unchanged for the case of the homogeneous transition, while the formula of $G_{\mathrm{ps}}(\omega_n, \mathbf{q})$ is somewhat modified. Since $G_{\mathrm{ps}}^{-1}(\omega_n, \mathbf{q})$ should have a minimum at $|\mathbf{q}| = 0$ in the homogeneous chiral transition, $\mathcal{O}(|\mathbf{q}|^2)$ is the leading term in $G_{\mathrm{ps}}^{-1}(\omega_n, \mathbf{q})$. Thus, the propagator for the homogeneous transition renders

$$G_{\mathrm{ps}}^{-1}(\omega_n, \mathbf{q}) \sim \tau + \bar{\gamma} |\mathbf{q}|^2 + a_1 |\omega_n| + a_2 \omega_n^2, \tag{36}$$

where

$$\bar{\gamma} \equiv \frac{d}{dq^2} G_{\mathrm{ps}}^{-1}(0, \mathbf{q}) \Big|_{|\mathbf{q}|=0}. \tag{37}$$

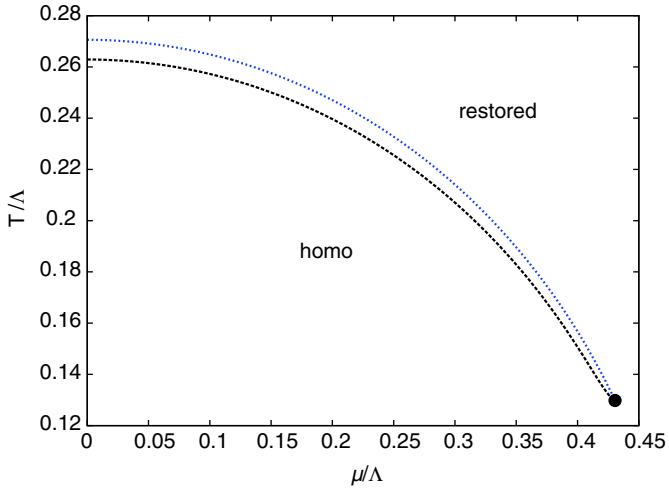


**Fig. 4.** Phase diagram including the chiral pair fluctuations of the homogeneous order parameter. The blue line denotes the phase boundary between the homogeneous broken and the chiral-restored phases in the MFA. The black line denotes the phase boundary including the fluctuation effects. The black dot is an endpoint of the homogeneous transition where the inhomogeneous condensate appears, which corresponds to the LP.

As in the previous section, we solve the Dyson–Schwinger equation represented in Fig. 1,

$$\tau \simeq \tau_R - \frac{\lambda}{4\pi^2}\left[\frac{1}{8\sqrt{a_2\bar{\gamma}}}\int_{1/\Lambda^2}^{\infty}\frac{dx}{x^2}e^{-\tau_R x/\bar{\gamma}} + \frac{\sqrt{a_2}}{\bar{\gamma}^{3/2}}\int_0^{\infty}dp\,\frac{p^2}{\sqrt{\tau_R/a_2+p^2}}\frac{1}{e^{\beta\sqrt{\tau_R/a_2+p^2}}+1}\right], \tag{38}$$

where we have used the PTR for the vacuum contribution. Here, since the numerical calculation shows that $a_1$ is sufficiently small, we have ignored $a_1|\omega_n|$ in $G_{\rm ps}^{-1}(\omega_n, \mathbf{q})$. Unlike the inhomogeneous case, we observe that the second term in the right-hand side of Eq. (38) remains finite even if $\tau_R$ is equal to zero. Thus, one may expect that the homogeneous transition remains of the second order, even though the chiral pair fluctuations are taken into account. Note that the order of the phase transition in this region is of the second order, which is suggested by the $O(4)$ universality in the Ginzburg–Landau–Wilson approach. Therefore, we consider the effect of the chiral pair fluctuations on the change of the phase boundary.

Instead of analytically carrying out the loop integral in Eq. (18), we here apply a rather simple way given in [7], which corresponds to the approximation of Eq. (18) up to $\mathcal{O}\left(q_c^2\right)$. Under the proper rescaling of the field variable, we find

$$\lambda = \frac{3g_{\phi qq}^{-4}N_f N_c}{\pi^2}\left[-1+\int_0^{\Lambda}\frac{dp}{p}\left(1-\frac{1}{e^{\beta(p-\mu)}+1}-\frac{1}{e^{\beta(p+\mu)}+1}\right)\right] \equiv 3\chi. \tag{39}$$

Figure 4 shows the phase diagram for the homogeneous chiral phase, containing the effect of the chiral pair fluctuations. Since $\lambda$ becomes small near the LP, the effect of fluctuations becomes small there. From this figure, we find that the effect of the chiral pair fluctuations reduces the size of the homogeneous phase. This is due to the enlargement of $\tau_R$ by the fluctuation effects as shown in Fig. 5.

We can see that both $\tau_R$ and $\tau$ monotonically decrease with decreasing temperature and eventually cross the zero line at a certain temperature. These crossing points correspond to the critical points for the second-order phase transition with or without fluctuations, which are denoted as $T_c$ and $T_c^{\rm MF}$. The blue line shows the temperature dependence of the difference $\Delta\tau = \tau_R - \tau$ as a criterion for evaluating the effect of the chiral pair fluctuations. Since $\Delta\tau$ monotonically decreases with increasing

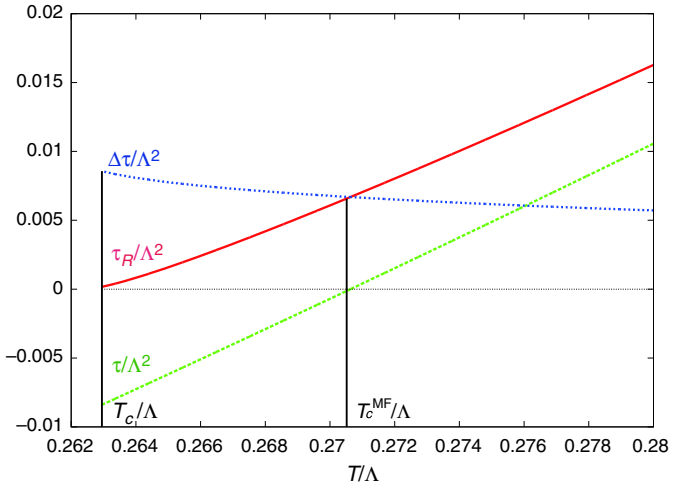


**Fig. 5.** Temperature dependence of $\tau$ and $\tau_R$ at $\mu/\Lambda = 0$ in the homogeneous order parameter. The red (green) line denotes the change of $\tau_R$ ($\tau$). The blue line denotes the difference $\Delta\tau = \tau_R - \tau$. In the horizontal axis, $T_c$ ($T_c^{\rm MF}$) represents the critical point with (without) the chiral pair fluctuations.

temperature, one may expect that thermal fluctuations become larger. However, the result exhibits the opposite behavior. This result can be understood by recalling that the coefficients of $G_{\rm ps}^{-1}(\omega_n, \mathbf{q})$ are the functions of temperature and chemical potential.

### *3.2. Inhomogeneous case*

Here we discuss the effect of the chiral pair fluctuations to the inhomogeneous chiral transition. First, restricting our discussion to the zero-temperature limit where the quantum fluctuations are dominant, we shall see that the quantum fluctuations change the order of the phase transition from the second to the first order by changing the sign of the fourth-order vertex function $\bar{\Gamma}^{(4)}$, while the quantum fluctuations to the second-order vertex function $\bar{\Gamma}^{(2)}$ move the phase boundary.

Next we discuss the fluctuation effects at finite temperature. Since the temperature dependence of the parameters dominates over the effect of the thermal fluctuations, we shall see that the phase boundary monotonically becomes close to that determined by the MFA as temperature increases.

In the following, we simply evaluate the formula of $\lambda$ as in the homogeneous case. A similar procedure can be done and we find $\lambda = -2\chi$ in the inhomogeneous case.

#### *3.2.1. $T = 0$*

We first discuss the effect of the quantum fluctuations to $\bar{\Gamma}^{(2)}$.

Here we show the behavior of $\tau$ as a function of $\tau_R$ in Fig. 6, where $\tau$ monotonically increases with increasing $\tau_R$. In particular, it diverges at $\tau_R \sim 0$ and never crosses with $\tau_R = 0$, so that $\tau_R$ is positive definite. This behavior implies that the phase transition never occurs as the second order. It is one of the differences from the study by Dyugaev [42], where only the possibility of the first-order phase transition is discussed. Such a behavior still remains in the high-temperature region.

Next we discuss the change of the location of the critical point by including the quantum fluctuations to $\bar{\Gamma}^{(2)}$. Figure 7 shows the chemical potential dependence of $\bar{\Gamma}^{(4)}$ at $T \sim 0$. From this figure, we find the red and green lines monotonically decrease with decreasing chemical potential, and eventually cross the zero line at a certain chemical potential denoted by $\mu_c$ and $\tilde{\mu}_c$.

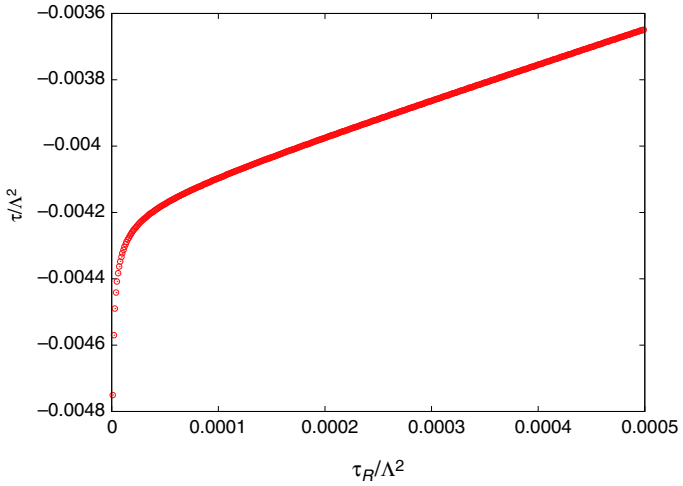


**Fig. 6.** $\tau_R$ dependence of $\tau$ at $T/\Lambda \sim 0$ and $\mu/\Lambda = 0.5566$.

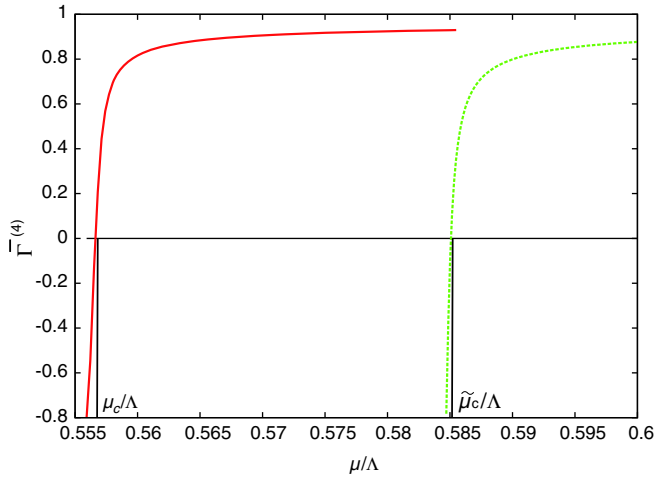


**Fig. 7.** Chemical potential dependence of $\bar{\Gamma}^{(4)}$ at $T/\Lambda \sim 0$. The red (green) line denotes $\bar{\Gamma}^{(4)}$ with (without) including the effect of the chiral pair fluctuations to $\bar{\Gamma}^{(2)}$. In the horizontal axis, $\mu_c$ ($\tilde{\mu}_c$) represents the critical point with (without) fluctuations.

The quantitative difference between $\mu_c$ and $\tilde{\mu}_c$ comes from the effect of the quantum fluctuations in $\bar{\Gamma}^{(2)}$; the inequality $\tau_R > \tau$ holds due to the quantum fluctuations, which implies that $L(0)$ becomes small. Since $\tau_R$ should be monotonically decreasing with decreasing chemical potential, we find that the phase boundary is shifted toward smaller chemical potential.

### *3.2.2.* $T > 0$

Finally, we discuss the termination boundary, taking into account the thermal fluctuations. As in the zero-temperature case, since the positiveness of $\tau_R$ also holds due to the third term in Eq. (29) and $\bar{\Gamma}^{(4)}$ becomes negative with $\tau_R \sim 0$, the chiral pair fluctuations change the order of the phase transition from the second to the first order at any temperature.

In Fig. 8, we present the phase diagram in the plane of temperature and chemical potential, taking into account the effect of the chiral pair fluctuations. As in the case of the homogeneous transition, the fluctuation effects reduce the inhomogeneous chiral phase. The effect of the chiral pair fluctuations

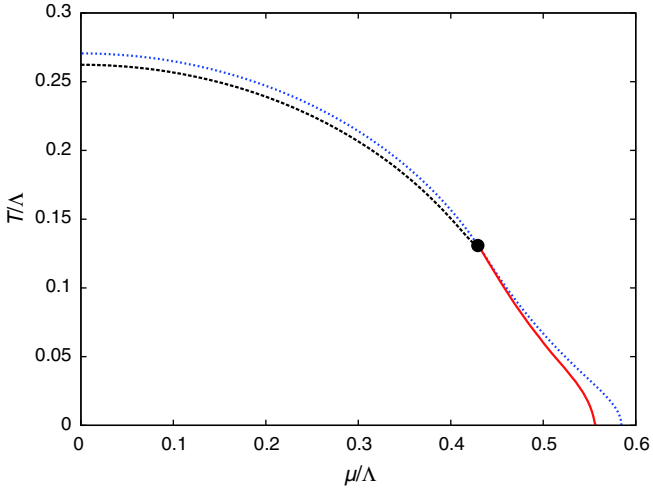


**Fig. 8.** Phase diagram in the plane of temperature and chemical potential, including the chiral pair fluctuation effects. The black dot represents the LP. The black and blue lines above the LP are the same as in Fig. 4. The blue (red) lines below the LP denote the phase boundary without (with) the effect of the chiral pair fluctuations.

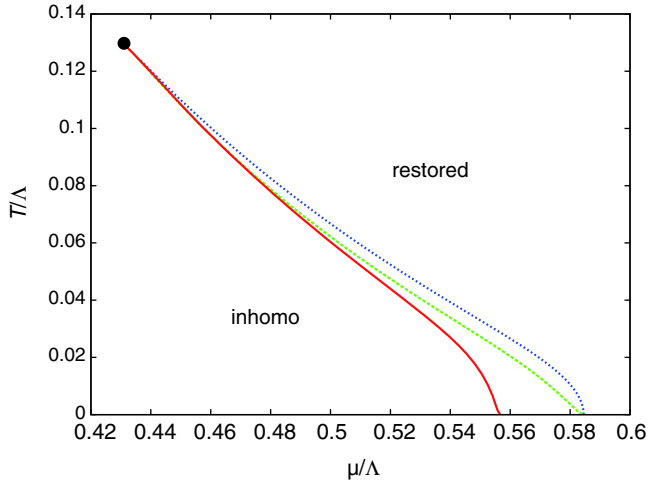


**Fig. 9.** The termination boundary obtained by including the chiral pair fluctuations. The black dot represents the LP. The blue line represents the first-order phase transition, including the quantum fluctuations to $\bar{\Gamma}^{(4)}$, which completely coincides with the second-order phase transition determined within the MFA. The green (red) line denotes the first-order phase transition, including the chiral pair fluctuations to $\bar{\Gamma}^{(4)}$ and thermal fluctuations (both quantum and thermal fluctuations) to $\bar{\Gamma}^{(2)}$.

to $\bar{\Gamma}^{(4)}$ gives rise to the sign change. Thus, unlike the homogeneous case, the fluctuation-induced phase boundary is of the first order.

In the following, we compare various fluctuation effects. Figure 9 shows the termination boundary for several cases by partially switching off the chiral pair fluctuations to $\bar{\Gamma}^{(2)}$ and/or $\bar{\Gamma}^{(4)}$.

If we only consider the quantum fluctuations to $\bar{\Gamma}^{(4)}$, which corresponds to the study by Dyugaev, the order of the phase transition changes from the second order to the first order (the blue line). On the other hand, the location of the phase boundary is unchanged from the one within the MFA. Thus, we find that the quantum fluctuations to $\bar{\Gamma}^{(4)}$ only change the order of the phase transition. We plot the phase boundary (the green line) by only including the thermal fluctuations to $\bar{\Gamma}^{(2)}$ and $\bar{\Gamma}^{(4)}$, which corresponds to the study by Brazovskii. From the comparison of the blue and green lines, it turns

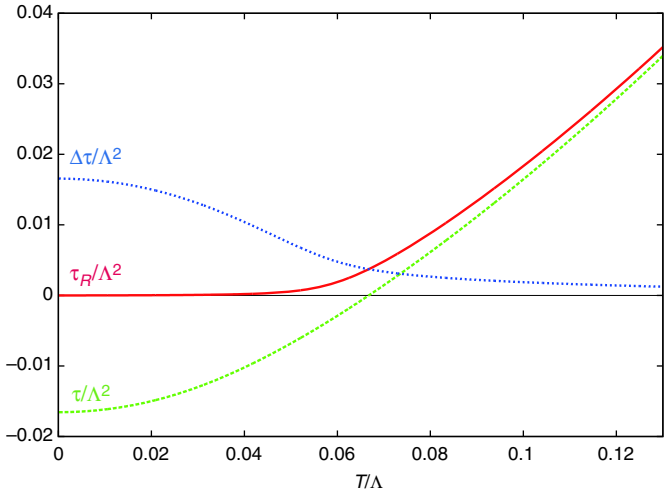


**Fig. 10.** Temperature dependence of $\tau$ and $\tau_R$ at $\mu/\Lambda = 0.5$ in the inhomogeneous order parameter. The red (green) line denotes the change $\tau_R$ ($\tau$). The blue line represents the difference $\Delta\tau = \tau_R - \tau$.

out that the inhomogeneous chiral phase is reduced by the thermal fluctuations. By including both quantum and thermal fluctuations to $\bar{\Gamma}^{(2)}$ and $\bar{\Gamma}^{(4)}$, we obtain the red line in Fig. 9. We see that the effect of the quantum fluctuations reduce the inhomogeneous chiral phase. From the comparison of the blue, green, and red lines, it turns out that the inclusion of the quantum fluctuations gives rise to the reduction of the inhomogeneous chiral phase in the low-temperature region. On the other hand, with increasing temperature, we find that the inclusion of the thermal fluctuations mainly reduces the inhomogeneous chiral phase. In particular, the inclusion of the quantum fluctuations to $\bar{\Gamma}^{(2)}$ is negligible around $T/\Lambda = 0.04$.

Since the thermal fluctuations should become large in the high-temperature region, it seems that our result is contrary to our naive thinking. However, we recall that the parameters in $G_{\rm ps}(\omega_n, \mathbf{p})$ are functions of temperature and chemical potential. For instance, the wave vector of the inhomogeneous condensate is monotonically decreasing with increasing temperature (or with decreasing chemical potential), so that this behavior should be dominant over the thermal fluctuations. Thus, we should take into account the change of the parameters to estimate the thermal-fluctuation effects. In order to measure these effects, we show the temperature dependence of the difference $\Delta\tau = \tau_R - \tau$ for fixed chemical potentials in Fig. 10.

The behaviors of $\tau$, $\tau_R$, and $\Delta\tau$ are qualitatively unchanged from the case of the homogeneous chiral phase, as in Fig. 5. In particular, $\Delta\tau$ is monotonically decreasing with increasing temperature. This implies that the change of the parameters dominates over the thermal fluctuations.

## 4. Summary and concluding remarks

In this paper, we have investigated the effect of the chiral pair fluctuations to the inhomogeneous chiral transition. In the MFA, the order of the phase transition is always of the second order, regardless of the function form of the inhomogeneous chiral condensate. In order to discuss both quantum and thermal fluctuations by considering the chiral pair excitations, we have formulated an effective action in terms of the composite fields made of the quark bilinear fields.

Starting from the effective action in the chiral-restored phase, which is a functional of the composite fields of quarks, we have constructed the thermodynamic potential. Since the order parameter is defined as the expectation value of the composite fields or the bilinear fields of quarks, the coefficients

of the thermodynamic potential (e.g., $\Gamma^{(2)}$ and $\Gamma^{(4)}$) should be described by the quark diagrams. Thus, we have introduced the propagator by considering the loop diagrams of the $q\bar{q}$ propagator in the NJL model. We have considered the effect of the chiral pair fluctuations to the second-order vertex function $\left(\bar{\Gamma}^{(2)}\right)$ and the fourth-order vertex function $\left(\bar{\Gamma}^{(4)}\right)$, and then have shown that our method incorporates both quantum and thermal fluctuations simultaneously. In particular, we have seen that terms given in the works by Brazovskii and Dyugaev are correctly reproduced in our formula, as a leading term of the thermal or vacuum fluctuations.

Further, we have presented some numerical results. In the beginning, we have discussed the chiral pair fluctuations in the homogeneous chiral transition. We have found that $\bar{\Gamma}^{(2)}$ approaches zero at finite temperature and chemical potential, where the susceptibility becomes divergent and it is a signal of the second-order phase transition. We have also found that the effect of the chiral pair fluctuations only moves the location of the phase boundary because the universality of the $O(4)$ symmetry ensures the order of the phase transition as second order in the homogeneous phase transition.

Next, we have discussed the effect of the chiral pair fluctuations in the inhomogeneous chiral phase. To begin with, we have discussed the zero-temperature limit in order to concentrate on the effect of the quantum fluctuations. We have found that $\tau_R$ decreases monotonically with decreasing chemical potential, but always stays positive. Thus we can conclude that the second-order phase transition is prohibited by the chiral pair fluctuations.

When $\tau_R$ becomes smaller, $\bar{\Gamma}^{(4)}$ decreases and eventually changes its sign. Thus, the order of the phase transition should change from the second to the first order. The location of the critical point is moved because of the effect of the quantum fluctuations to $\bar{\Gamma}^{(2)}$, whereas the location is not moved if we only consider the effect to $\bar{\Gamma}^{(4)}$. Subsequently, we have discussed the effects of the thermal fluctuations. The effects are qualitatively the same as the quantum fluctuations: $\tau_R$ is positive definite and $\bar{\Gamma}^{(4)}$ changes its sign. Finally, we have considered both fluctuation effects in the temperature–chemical potential plane. We have observed that both fluctuations to each vertex function change the order of the phase transition and reduce the region of the inhomogeneous chiral phase at any temperature. In the low-temperature region, the thermal fluctuations to both vertexes are small compared to the quantum fluctuations to $\bar{\Gamma}^{(2)}$, while it becomes predominant with increasing temperature.

There remain some interesting subjects in connection with our study. It is important to find some thermodynamic quantities characterized by the nature of the first-order phase transition. Typically, there are some quantities such as entropy or latent heat that are discontinuous at the phase boundary. In this paper, we have discussed the effect of the chiral pair fluctuations based on the resummation of the diagram. A more sophisticated approach might be needed to confirm our findings and extract more information about the fluctuation-induced first-order phase transition. For instance, Ling et. al. [54] have discussed the inhomogeneous phase transition in some simple models with the help of the renormalization group (RG) method. We expect the RG method can also be applied in the context of the inhomogeneous chiral transition.

**Acknowledgement**

This work is supported by Grant-in-Aid for Scientific Research on Innovative Areas from MEXT (Grant No. 24105008).

## Appendix A. Derivation of Eqs. (7) and (8)

Here we derive the propagator. In the following, $\omega_n$ ($\tilde{\omega}_m$) represents the Matsubara frequency for bosonic (fermionic) fields. Hereafter, we restrict $\omega_n$ to the positive frequency. In order to evaluate

Eq. (6), we use the retarded/advanced Green's function in real time, which is defined by

$$S_{R/A}(\omega, \mathbf{q}) = -\int_{-\infty}^{\infty} dp_0 \frac{\left(p_0'\gamma_0 - \vec{\gamma}\cdot\mathbf{q}\right)\epsilon\left(p_0'\right)\delta\left(p_0'^2 - \mathbf{q}^2\right)}{\omega - p_0 \pm i\varepsilon}, \tag{A1}$$

where $p_0' = p_0 + \mu$ and $\varepsilon$ is an infinitesimal number. Here, $S_{R/A}$ is closely related to the thermal Green's function,

$$S_\beta(\tilde{\omega}_m, \mathbf{q}) = S_R(i\tilde{\omega}_m, \mathbf{q}). \tag{A2}$$

Using the equality of Eq. (A2) and performing the fermionic Matsubara frequency sum, we can rewrite Eq. (6) as

$$\begin{aligned}\Pi^0_{\rm ps}(\omega_n, \mathbf{q}) = \int \frac{d^4p}{(2\pi)^4} \tanh\frac{\beta p_0}{2} \mathrm{tr}\Big[ & S_R(p_0 + i\omega_n, \mathbf{p}+\mathbf{q})\mathrm{Im}S_R(p_0, \mathbf{p}) \\ & + S_A(p_0 - i\omega_n, \mathbf{p}-\mathbf{q})\mathrm{Im}S_R(p_0, \mathbf{p})\Big].\end{aligned} \tag{A3}$$

For the first and second terms, a straightforward calculation yields the following results:

$$\begin{aligned}&\int \frac{d^4p}{(2\pi)^4} \tanh\frac{\beta p_0}{2} \mathrm{tr}\Big[ S_R(p_0 + i\omega_n, \mathbf{p}+\mathbf{q})\mathrm{Im}S_R(p_0, \mathbf{p})\Big] \\ &= -\frac{1}{2}\frac{N_f N_c}{(2\pi)^2}\int_{-1}^{1} dx \int_0^\infty pdp \left[\tanh\frac{\beta(p-\mu)}{2}\left(1 - \frac{-\omega_n^2 - |\mathbf{q}|^2}{-\omega_n^2 - |\mathbf{q}|^2 - 2p|\mathbf{q}|x + 2ip\omega_n}\right)\right. \\ &\quad \left. - \tanh\frac{\beta(-p-\mu)}{2}\left(1 - \frac{-\omega_n^2 - |\mathbf{q}|^2}{-\omega_n^2 - q^2 - 2p|\mathbf{q}|x - 2ip\omega_n}\right)\right],\end{aligned} \tag{A4}$$

$$\begin{aligned}&\int \frac{d^4p}{(2\pi)^4} \tanh\frac{\beta p_0}{2} \mathrm{tr}\Big[ \mathrm{Im}S_R(p_0, \mathbf{p}) S_A(p_0 - i\omega_n, \mathbf{p}-\mathbf{q})\Big] \\ &= -\frac{1}{2}\frac{N_f N_c}{(2\pi)^2}\int_{-1}^{1} dx \int_0^\infty pdp \left[\tanh\frac{\beta(p-\mu)}{2}\left(1 - \frac{-\omega_n^2 - |\mathbf{q}|^2}{-\omega_n^2 - |\mathbf{q}|^2 + 2p|\mathbf{q}|x + 2ip\omega_n}\right)\right. \\ &\quad \left. - \tanh\frac{\beta(-p-\mu)}{2}\left(1 - \frac{-\omega_n^2 - |\mathbf{q}|^2}{-\omega_n^2 - |\mathbf{q}|^2 + 2p|\mathbf{q}|x - 2ip\omega_n}\right)\right].\end{aligned} \tag{A5}$$

Substituting Eqs. (A4) and (A5) into Eq. (A3) and performing the PTR for the vacuum contribution, we obtain Eqs. (7) and (8).

## Appendix B. Correlation function method

We briefly review the correlation function method [4] to analyze the second-order phase transition. The function form of the static polarization function $\Pi^0_{\rm ps}$ at finite temperature and chemical potential is given by

$$\begin{aligned}\Pi^0_{\rm ps}(0, \mathbf{q}) &\equiv T\sum_m \int \frac{d^3p}{(2\pi)^3} \mathrm{tr}\left[i\gamma_5\tau_3 S_\beta(\tilde{\omega}_m, \mathbf{q}+\mathbf{p})\, i\gamma_5\tau_3 S_\beta(\tilde{\omega}_m, \mathbf{p})\right] \\ &= \frac{N_f N_c}{(2\pi)^2}\Lambda^2 - 2iN_f N_c|\mathbf{q}|^2 I\left(|\mathbf{q}|^2\right) \\ &\quad + \frac{N_f N_c}{2\pi^2}\int_0^\infty pdp\, \frac{1}{e^{\beta(p+\mu)}+1}\left(2 - \frac{|\mathbf{q}|}{2p}\log\left|\frac{|\mathbf{q}|+2p}{|\mathbf{q}|-2p}\right|\right) \\ &= \Pi^{0,\rm vac}_{\rm ps}(0, \mathbf{q}) + \Pi^{0,\rm med}_{\rm ps}(0, \mathbf{q}),\end{aligned} \tag{B1}$$

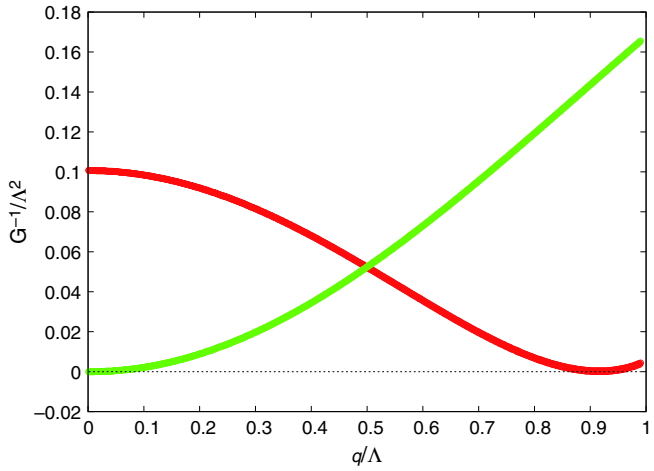


**Fig. B1.** Function $G_{\rm ps}^{-1}(0,\mathbf{q})$ versus momentum $q$ near the phase boundary. The red (green) line denotes the phase boundary between the inhomogeneous (homogeneous) chiral and chiral-restored phases at $T/\Lambda = 0.001(0.27)$ and $\mu/\Lambda = 0.5845(0)$ with $\Lambda = 660.37$ MeV.

where $S_\beta$ is the thermal quark propagator and $\Lambda$ an ultraviolet cutoff. Here, $I\left(|\mathbf{q}|^2\right)$ is defined as

$$I\left(|\mathbf{q}|^2\right) \equiv \frac{i}{16\pi^2}\int_0^1 dt \int_{1/\Lambda^2}^{\infty} \frac{d\tau}{\tau}\, e^{-|\mathbf{q}|^2 t(1-t)\tau}, \tag{B2}$$

where the vacuum contribution has been regularized with the PTR scheme. Expanding the logarithmic function of $|\mathbf{q}|$ in Eq. (B1), one can easily find that $\Pi_{\rm ps}^{0.\rm med}(0,\mathbf{q})$ is an even function of $|\mathbf{q}|$.

If the phase transition is of the second order, the minimum of $\Gamma_{\rm ps}^{(2)}(0,\mathbf{q})$ is always positive in the chiral-restored phase. At fixed $T$, the minimum monotonically decreases with decreasing $\mu$ and eventually reaches zero. At this point the susceptibility diverges with a finite momentum, and thus the phase transition occurs between the inhomogeneous chiral and the chiral-restored phase. Consequently, the following specific conditions are obtained:

$$1 - 2G\Pi_{\rm ps}^0(0,\mathbf{q}) = 0 \quad \text{and} \quad \partial_q \Pi_{\rm ps}^0(0,\mathbf{q}) = 0. \tag{B3}$$

Figure B1 shows the typical behavior of the static propagator, $G_{\rm ps}(0,\mathbf{q})$, near the phase boundary. Note that $G_{\rm ps}^{-1}$ has a minimum with finite momentum near the phase boundary between the inhomogeneous chiral and chiral-restored phases, while it takes a minimum with zero momentum near the phase boundary between the homogeneous chiral and chiral-restored phases.

## Appendix C. Matsubara frequency sum of the last term in Eq. (28)

We perform the Matsubara frequency sum given by

$$T\sum_n G_{\rm ps}^R(\omega_n,\mathbf{p}) = TG_{\rm ps}^R(0,\mathbf{p}) + 2T\sum_{n=1}^{\infty}\frac{1}{\eta + a_1|\omega_n| + a_2\omega_n^2}, \tag{C1}$$

where $\eta \equiv \tau_R + \gamma\left(|\mathbf{p}|^2 - q_c^2\right)^2$. Here we take the Matsubara frequency sum in the second term. In the following, we denote the solution of the equation $\eta + a_1 x + a_2 x^2 = 0$ by $\kappa_\pm$. From the numerical results we find that $a_1$ and $\eta$ are always positive and $a_2$ is always negative.

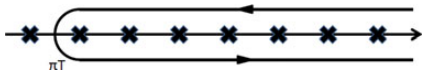


**Fig. C1.** Contour of the integral with the Matsubara frequency sum.

Considering the contour as in Fig. C1, we perform the Matsubara frequency sum:

$$T\sum_{n=1}^{\infty}\frac{1}{\eta+a_1|\omega_n|+a_2\omega_n^2}=\int_{i\infty+\pi T}^{-i\infty+\pi T}\frac{dz}{2\pi}\frac{1}{e^{iz/T}+1}\frac{1}{\eta+a_1z+a_2z^2}. \tag{C2}$$

Here, since there is one pole in the positive real axis, we should consider the contribution from it. Thus, we regard $\kappa_+$ as a pole of the integrand in the positive real axis.

If $\kappa_+$ is smaller than $\pi T$, we do not have to consider the contribution from the pole $\kappa_+$ and hence obtain Eq. (29). If $\kappa_+$ is larger than $\pi T$, on the other hand, we should consider the contribution from the pole $\kappa_+$ by performing the Matsubara frequency sum,

$$\begin{aligned}T\sum_{n=1}^{\infty}\frac{1}{\eta+a_1|\omega_n|+a_2\omega_n^2}&=-\frac{2}{a_2}\int_0^{\infty}\frac{dz}{2\pi}\tanh\frac{z}{2T}\frac{\sigma z}{\left[z^2+(\sigma+\rho)^2\right]\left[z^2+(\sigma-\rho)^2\right]}\\&\quad-i\mathrm{Res}_{z\to\kappa_+}\frac{1}{a_2(z-\kappa_+)(z-\kappa_-)}\frac{1}{e^{iz/T}-1}\\&=-\frac{2}{a_2}\int_0^{\infty}\frac{dz}{2\pi}\tanh\frac{z}{2T}\frac{\sigma z}{\left[z^2+(\sigma+\rho)^2\right]\left[z^2+(\sigma-\rho)^2\right]}\\&\quad+\frac{1}{2\sqrt{a_1^2-4a_2\eta}}\cot\frac{\kappa_+}{2T},\end{aligned} \tag{C3}$$

where $\sigma$ and $\rho$ are defined by

$$\sigma=-\frac{a_1}{2a_2}-\pi T, \tag{C4}$$

and

$$\rho=\frac{\sqrt{a_1^2-4a_2\eta}}{2a_2}. \tag{C5}$$

Here, since $\eta$ and $\kappa_+$ depend on the momentum, we find that the last term in Eq. (C3) oscillates rapidly in the momentum space and is almost canceled out in each period in the momentum integration. Thus, we obtain the result given in Eq. (29), assuming that the contribution from the last term in Eq. (C3) can be negligible.

## References

[1] K. Fukushima and C. Sasaki, Prog. Part. Nucl. Phys. **72**, 99 (2013).
[2] D. V. Deryagin, D. Yu. Grigoriev, and V. A. Rubakov, Int. J. Mod. Phys. A **7**, 659 (1992).
[3] E. Shuster and D. T. Son, Nucl. Phys. B **573**, 434 (2000).
[4] E. Nakano and T. Tatsumi, Phys. Rev. D **71**, 114006 (2005).
[5] G. Basar and G. V. Dunne, Phys. Rev. Lett. **100**, 200404 (2008).
[6] G. Basar, G. V. Dunne, and M. Thies, Phys. Rev. D **79**, 105012 (2009).
[7] D. Nickel, Phys. Rev. D **80**, 074025 (2009).
[8] D. Nickel, Phys. Rev. Lett. **103**, 072301 (2009).
[9] T. Kojo, Y. Hidaka, L. McLerran, and R. D. Pisarski, Nucl. Phys. A **843**, 37 (2010).
[10] S. Carignano, D. Nickel, and M. Buballa, Phys. Rev. D **82**, 054009 (2010).
[11] H. Abuki, D. Ishibashi, and K. Suzuki, Phys. Rev. D **85**, 074002 (2012).

[12] D. Müller, M. Buballa, and J. Wambach, Phys. Lett. B **727**, 240 (2013).
[13] A. W. Overhauser, Phys. Rev. Lett. **4**, 462 (1960).
[14] A. W. Overhauser, Phys. Rev. **128**, 1437 (1962).
[15] G. Grüner, Rev. Mod. Phys. **60**, 1129 (1988).
[16] G. Grüner, Rev. Mod. Phys. **66**, 1 (1994).
[17] P. Fulde and R. A. Ferrell, Phys. Rev. **135**, A550 (1964).
[18] A. I. Larkin and Y. N. Ovchinnikov, Zh. Eksp. Teor. Fiz. **47**, 1136 (1964).
[19] M. Buballa and S. Carignano, Prog. Part. Nucl. Phys. **81**, 39 (2015).
[20] J. Moreira, B. Hiller, W. Broniowski, A. A. Osipov, and A. H. Blin, Phys. Rev. D **89**, 036009 (2014).
[21] H. Abuki, Phys. Rev. D **87**, 094006 (2013).
[22] H. Abuki, Phys. Lett. B **728**, 427 (2014).
[23] D. Nowakowski, M. Buballa, S. Carignano, and J. Wambach, [arXiv:1506.04260 [hep-th]] [Search INSPIRE].
[24] M. Buballa and S. Carignano, [arXiv:1508.04361 [nucl-th]] [Search INSPIRE].
[25] S. Carignano, E. J. Ferrer, V. de la Incera, and L. Paulucci, Phys. Rev. D **92**, 105018 (2015).
[26] O. Schnetz, M. Thies, and K. Urlichs, Ann. Phys. **321**, 2604 (2006).
[27] S. Maedan, Prog. Theor. Phys. **123**, 285 (2010).
[28] V. Schön and M. Thies, Phys. Rev. D **62**, 096002 (2000).
[29] S. Karasawa and T. Tatsumi, Phys. Rev. D **92**, 116004 (2015).
[30] I. E. Frolov, V. Ch. Zhukovsky, and K. G. Klimenko, Phys. Rev. D **82**, 076002 (2010).
[31] K. Nishiyama, S. Karasawa, and T. Tatsumi, Phys. Rev. D **92**, 036008 (2015).
[32] T. Tatsumi, K. Nishiyama, and S. Karasawa, Phys. Lett. B **743**, 66 (2015).
[33] G. Basar and G. V. Dunne, Phys. Rev. D **78**, 065022 (2008).
[34] R. Yoshiike, K. Nishiyama, and T. Tatsumi, Phys. Lett. B **751**, 123 (2015).
[35] L. D. Landau and E. M. Lifshitz, *Statistical Physics* (Pergamon Press, Oxford, 1969).
[36] T.-G. Lee, E. Nakano, Y. Tsue, T. Tatsumi, and B. Friman, Phys. Rev. D **92**, 034024 (2015).
[37] Y. Hidaka, K. Kamikado, T. Kanazawa, and T. Noumi, Phys. Rev. D **92**, 034003 (2015).
[38] S. A. Brazovskii, Sov. Phys. J. Exp. Theor. Phys. **41**, 85 (1975).
[39] L. Leibler, Macromolecules **13**, 1602 (1980).
[40] D. Brisbin, D. L. Johnson, H. Fellner, and M. E. Neubert, Phys. Rev. Lett. **50**, 178 (1983).
[41] F. S. Bates, J. H. Rosedale, G. H. Fredrickson, and C. J. Glinka, Phys. Rev. Lett. **61**, 2229 (1988).
[42] A. M. Dyugaev, J. Exp. Theor. Phys. Lett. **22**, 83 (1975).
[43] Y. Nambu and G. Jona-Lasinio, Phys. Rev. **124**, 246 (1961).
[44] A. Altland and B. Simons, *Condensed Matter Field Theory* (Cambridge University Press, Cambridge, 2006).
[45] H. Orland and J. W. Negele, *Quantum Many-Particle Systems* (Westview Press, Boulder, CO, 1998).
[46] S. P. Klevansky, Rev. Mod. Phys. **64**, 649 (1992).
[47] H. Sugawara and T. Eguchi, Phys. Rev. D **10**, 4257 (1974).
[48] K. Kikkawa, Prog. Theor. Phys. **56**, 947 (1976).
[49] A. B. Migdal, Rev. Mod. Phys. **50**, 107 (1978).
[50] H. Kleinert, Phys. Lett. B **102**, 528 (1981).
[51] K. Kolehmainen and G. Baym, Nucl. Phys. A **382**, 528 (1982).
[52] Y. Ohashi, J. Phys. Soc. Jpn. **71**, 2625 (2002).
[53] G. H. Fredrickson and K. Binder, J. Chem. Phys. **91**, 7265 (1989).
[54] D. D. Ling, B. Friman, and G. Grinstein, Phys. Rev. B **24**, 2718 (1981).